Mehran University Research Journal of Engineering and Technology

https://doi.org/10.22581/muet1982.2203.06

2022, 41(3) 54-71

Comparison of solving probabilistic optimal power flow methods in the presence of wind and solar sources

Hamid Fattahi [a], Hamdi Abdi [b], Farshad Khosravi [a,*], Shahram Karimi [b]

[a] *Department of Electrical Engineering, Kermanshah Branch, Islamic Azad University, Kermanshah, Iran*

[b] *Department of Electrical Engineering, Engineering Faculty, Razi University, Kermanshah, Iran*

[*] Corresponding Author: Farshad Khosravi, Email: farshad.khosravi.iau@gmail.com

Received: 25 July 2020, Accepted: 25 February 2022, Published: 01 July 2022

K E Y W O R D S

Uncertainty

Probabilistic Optimal Power Flow (POPF)

Renewable Energy Sources

Monte Carlo Simulation (MCS)

3 Point Estimation Method (3PEM)

Unscented Transformation (UT)

Interior Point Method (IPM)

A B S T R A C T

Power system control and operation studies have been experienced essential changes due to increasing the penetration of uncertain renewable energy resources. One of the most critical issues in this regard is the optimal power flow (OPF). As a result, the deterministic methods do not have the capability of different modeling uncertainties raised in new power systems, and there is a need to investigate the effective models in this regard. This paper focuses on probabilistic optimal power flow (POPF) methods applied to power systems with uncertain wind and Photovoltaic power generations. In this paper, the Monte Carlo simulation (MCS) and analytical methods such as the three-point estimation method (3PEM), unscented transformation (UT), and Interior-Point method (IPM) are applied to solve the probabilistic optimal power flow problem. MCS has been widely applied as a framework to assess the ability of analytical methods. The mentioned techniques are applied to a sample case study extracted from the IEEE 300-bus system. The main contribution of this work is the comparison of analytical methods concluding 3PEM, UT, and IPM, and with MCS as well. The obtained results on the studied networks by the suggested techniques show that in the 3PEM, due to the limited points, the optimal solution is achieved in less calculation time than the other methods. From another perspective, the voltage changes at the buses would be more stable in the IPM. Also, this method is much faster than the MCS method in terms of the convergence rate. To show the effectiveness of the mentioned methods, this paper presents probabilistic load flow method based on the statistical methods to deal with fluctuations because of large-scale renewable energy integration. The proposed methods are validated on the improved industrial 85–bus system of Kermanshah region (in the west of Iran) by adding solar and wind farms.

1. Introduction

Replacing fossil fuels with renewable energy resources is inevitable due to environmental concerns. Wind and solar power are the dominant technologies in this context [1]. Because of the uncertain behavior of renewable energies, it is necessary to use suitable methods [2]. POPF analysis is one of the essential tools in this field.

Power Flow (PF) analysis determines load, generation, and the other electrical variables based on system conditions. The most critical uncertainties in the power system are mainly related to the restructuring of the power system as well as to the unprecedented use of renewable energy. In such systems, the calculation of the Deterministic Optimal Power Flow (DOPF) cannot describe the actual status of the power system. The probabilistic analysis then becomes necessary. POPF analysis is one of the basic tools in the operation and control of uncertain power systems. The history of research in this field is mainly referred to as the early 1970s [3].

Probabilistic power transmission can accurately examine the state of the power system and calculate base voltages and line conditions in the presence of uncertainty, so this method can provide useful information for researchers for making necessary decisions on the power system. The green-house side effects and environmental concerns are becoming more critical. As a result, and as a relatively clean and renewable energy generation, wind power plants and solar panels are being focused on by researchers and operators. However, these technologies pose significant challenges and problems to power system operation and control due to their uncertain inputs. So, it is essential to consider the probabilistic models to ensure safety and stability [4].

Wind power plants as a clean and environmentally friendly generation are increasingly integrated into the power systems more and more. As a result, the impacts of relevant uncertainties on power system planning, operation, and control should be taken in10to account. In this context, POPF results provide some comprehensive references for electricity researchers, planners, and operators to make an accurate decision based on this uncertain analysis. Therefore, it is essential to investigate POPF considering relevant uncertainties as well as their mutual dependence [5].

There are several methods for solving optimal probability flow, including MCS, the PEM, IPM, and UT methods. Although MCS gives accurate values based on random sampling, it is very time-consuming and is therefore not suitable for large systems. PEM has high efficiency and high accuracy in calculating an average and standard deviation [6]. Last, UT is a recently proposed method with excellent performance in nonlinear modes compared to the estimation method presented in [7]. This method has a high computation accuracy and is considerably faster than the MCS method. One of the advantageous features of the UT method is the possibility of modeling the uncertainty variables directly. To investigate uncertainty in the wind power system, the Weibull distribution of [8-10] and the Rayleigh distribution [10] are used. Then, the active power injected by the wind power system is calculated using the generator's power and speed ratio.

The correlation between wind generators and power plants is considered [10-14]. In the literature, it seems that no model has considered this uncertainty in its direct form [1]. To investigate the uncertainty associated with solar energy, the beta distribution is used, using which we can calculate the injection power of the solar cell [15]. Analytical methods are applied based on a set of mathematical assumptions and relatively complex algorithms. In the case of using Probabilistic Power Flow Analysis, the following shortcomings are probable: The Jacobean matrix should be calculated during linearization, which might be a problematic and process and prone to errors. The linearization transformation is reliable when we approximate the error propagation by applying some linear functions. Therefore, the new analysis methods for nonlinear probabilistic systems are essential, having a high level of accuracy, having a suitable run time for each issue, ease of use, and the possibility of managing the correlated variables.

A new PEM was used for probabilistic calculations to calculate the probabilistic power flow [16]. The two-PEM was used as an articular version of the PEM for examining the optimal probability distribution in [16]. The calculation time for the PEM and its different versions are proportional to the dimensions of the problem and the number of uncertainties, which may make this method inefficient for large-scale problems. To meet the requirements of the analytical methods, a new nonlinear transformation method and the covariance of output variables were used in [16]. The UT method has high computational accuracy and is considerably faster than the MCS method. One of the practical features of the UT method is the possibility of modeling the uncertainty variables directly. A new approach is proposed to conduct a probabilistic study based on the PEM [17-19]. This method also was proposed to investigate the optimal probability distribution in [20]. Two distinct mathematical methods for managing variables were suggested using the PEM [21-22]. However, it was claimed that PEM is not appropriate for large-scale problems with high levels of uncertainty [20].

The internal point method for solving the optimization problems is based on constructing a path

from a given point to search for the final solution in a possible region. This method was firstly proposed in 1984 [23] and has since been investigated in several studies [24]. This method has been used in various fields of power system operation such as economic load dispatch security-constrained optimal power flow, assessment of power system load-ability, and loss reduction [25]. This method is often used to solve linear optimization problems such as transmission expansion planning [26]. The main weakness of the internal point method is when the active constraints prevent the point from reaching the zero point or the acceptable boundary. Therefore, the great challenge in applying this method to solving the optimal power flow problem is to introduce a robust convergence approach to show the current limitations to prevent inefficiency. To deal with this problem in [27], some guidelines were discussed. The penalty function method is used to solve the nonlinear optimization problem in which a quadratic approximation is used to solve the internal point method problem [28].

Probability theory is used to indicate the uncertainty of optimal power flow [29]. A fuzzy-based optimization approach is proposed to schedule the generation in power systems considering various uncertainties [30]. Addressed the different types of probabilistic uncertainties in load-flow studies in the modern power system [31].

The point estimation method has been expanded using random variables with an arbitrary distribution in the probability optimal power flow [32]. Presented a method for combining (1+2m) to investigate the impacts of different random inputs concluding spatial and temporal variables [33]. Also, a modified PEM is analyzed POPF problem considering the correlation between sole, wind as well as the demanded loads [9, 21].

The OPF problem has been studied in a multi-objective optimization framework [34]. Also, investigating this complex problem in the stochastic condition in the presence of random variables arising from wind and solar energy resources and their correlation by using the probability density functions is of great importance. The authors in [35] have addressed this concept by applying the MCS method. Two MCS methods are proposed, along with the point estimation method [36].

The MCS method is usually a basic framework for POPF since it uses the real nonlinear power flow equations, and it is simple to expand. The answers to this method are used as a benchmark. MCS is among the widely applied numerical methods for POPF. Analytical solutions provide another option for solving POPF using probability densities. A PEM is a solution option for a probabilistic problem that operates with random variables [37]. PEM is considered a state-of-the-art method for solving OPF problems with accuracy and efficiency. Rosenblueth modified the PEM as 2 m [17].

Probabilistic methods, including the MCS Method and the PEM, have been used [38]. By using the MCS Method, we can achieve the exact voltage and power flow of branches. PEM is widely used to distribute the probability of the optimal probability flow problem, which can be used to calculate the significant statistical results of a deterministic optimal flow [37].

PEM for analyzing the statistical moments of a random value as a function of "m input random variables" is proposed. The load is modeled as a random variable, and two individual cases of PEM concluding $2m$ and $2m+1$ concentration schemes were considered [39]. In the $2m$ scheme, only the skewness is considered, but in the $2m+1$ scheme, both skewness and kurtosis are mentioned in PDF. As the value of a random variable change based on predetermined distribution, the expected values for voltage of the buses and line loading are determined. Also, the results of deterministic PLF are entirely compared with the obtained results applying $2m$ and $2m+1$ scheme.

We have modeled the wind speed as a Weibull distribution using actual data and normal distributions for modeling the demanded loads [40]. The PEMs are compared with MCS results. As it was reported in this reference, the PEMs reach acceptable results in acceptable calculation time. However, in some conditions, PEMs may give inaccurate results.

Combined Zhao's PEM with Nataf transformation and applied the combined method to solve the correlated PLF [9]. As it was stated in that reference, the mentioned technique can quickly deal with correlated input random variables in non-normal and normal Probability Density Functions (PDFs).

Applied power system graph in which a novel probabilistic strategy for generating all probable islanding solutions are mentioned, and they are reduced using different evaluating static and dynamic constraints they are reduced [41]. The presented technique considers the relevant uncertainties to the wind farm and demanded loads and analyzed the steady-state stability of all partitions in each possible solution.

A probabilistic multi-objective OPF concluding the load and wind speed correlations is presented [2]. It applied a PEM based on Nataf transformation. Furthermore, Hong's PEM as a popular tool is applied to deal with uncertainty. Both and schemes of Hong's PEM have been analyzed, and the obtained results are compared with MCS [42].

The most important contributions of this paper are highlighted as under.

1. Applying three analytical methods of PEMs based on three points, UT and IPM, to POPF problem.
2. Comparing the obtained results of above-mentioned techniques with the standard MCS method.
3. Reporting the simulation results on the 300-bus IEEE case study, as a large-scale power system.
4. Demonstrating the obtained results on an improved industrial 85–bus system of Kermanshah region (in the west of Iran), as a practical case study.

Investigating and comparing the methods in terms of accuracy, convergence of the optimal solutions, the value of objective function and run-time.

2. The Problem Formulation

The optimal power flow is a nonlinear optimization problem and its primary purpose is minimizing the fuel cost of power plants taking into account the equality and inequality constraints.

One of the most important goals of the OPF problem is to minimize the fuel cost of generators. To achieve this goal, the quadratic Eq. 1 is used [43].

$$f(x,u) = \sum_{i=1}^{NG} a_i + b_i P_{G_i} + c_i P_{G_i}^2 \quad (1)$$

Where, a_i, b_i and c_i are the generator's cost coefficients for ith generator, with the output power of P_{G_i}. The OPF is an optimization problem with a single-objective function that serves to minimize the cost of exploitation [44].

Any external parameter may affect the parameters of the power system and apply uncertainty to the system. To evaluate the uncertainty of a system, probability theory is employed in the form of probabilistic methods to define the status of the power system.

2.1 Modeling Methods for POPF

2.1.1 Numerical method

MCS is one of the precise random methods. The MCS, as an approach independent of the size of the system, is used for a complex and nonlinear system that contains uncertain variables [45]. The MCS is based on the repetition, which is as follows.

Step 1: Set Monte Carlo simulator counter $c = 1$,

Step 2: Generate random sample vector x by using probability density function for each component x_i,

Step 3: Calculate $y = f(x_i)$ assuming $x = x_c$,

Step 4: Calculate the mean value of y applying $E(y) = \frac{\sum_c y_c}{c}$,

Step 5: Calculate the variance y by $\sigma(y) = E(y^2) - E^2(y)$,

Step 6: Stop the process, and end or count at $c = c + 1$ and return to Step 2,

Step 7: End [5].

2.1.2 Analytical methods

Analytical methods are based on the approximation of PDFs. This process is more straightforward than the approximation of the nonlinear transformation function. The basis of these methods is how to produce suitable examples of input variables that can obtain sufficient information about the PDF.

2.1.2.1 Three-PEM

In this technique, h is the number of points in the estimated PDF. The general theory of the method h is in [46]. However, a three-PEM is used in this work, and the probabilistic optimal power flow method by using this method is given as below.

The estimation method from 3 to h points, which is estimated by Eq. 2, is as under.

$$x_{l.k} = \mu_l + \xi_{l.k}\sigma_l \quad (2)$$

Where μ_l and σ_l are, respectively, the mean and standard deviation of $x_{l,k}$. $\xi_{l.k}$ can be obtained in two parts of the method of 3 to h points. The three PEM for each variable x_l with their respective weights is described as follows.

Using the skewness and kurtosis coefficients, x_l can be calculated from Eq. 3 and Eq. 4, respectively.

$$\lambda_{l.3} = \frac{E[(x_l - \mu_l)^3]}{\sigma_l^3} \quad (3)$$

$$\lambda_{l.4} = \frac{E[(x_l - \mu_l)^4]}{\sigma_l^4} \quad (4)$$

Where $E[(x_l - \mu_1)^P] = \sum_{t=1}^{N}(x_1(t) - \mu_1)^P \times P_r(x_1(t))$, P = 3 or 4. N is the number of observations for $x_1(t)$ the value of t is the observation of x_l and $P_r(x_1(t))$ is the probability $x_1(t)$.

In Eq. 5, we can obtain $\xi_{l.1}$ and $\xi_{l.2}$, whereas $\xi_{l.3} = 0$.

$$\xi_{l.k} = \frac{\lambda_{l.3}}{2} + (-1)^{3-k} \times \sqrt{\lambda_{l.4} - \frac{3}{4}\lambda_{l.3}^2}\,.k \quad (5)$$
$$= 1.2$$

To estimate the density function, the probability of estimating the three points of $y = f(x)$ is used. Also, the values of the weight coefficients $w_{l.1}$. $w_{l.2}$, and $w_{l.3}$ are obtained using Eqs. 6 and 7.

$$w_{l.k} = \frac{(-1)^{3-k}}{\xi_{l.k}(\xi_{l.1} - \xi_{l.2})}\ .\ k = 1.2 \quad (6)$$

$$w_{l.3} = \frac{1}{n} - \frac{1}{\lambda_{l.4} - \lambda_{l.3}^2} \quad (7)$$

2.1.2.2 Unscented transformation method

The Unscented Transformation (UT) method was introduced to overcome the drawbacks of ordinary probabilistic methods, especially those that used the linearization process. Analytical methods are developed based on some mathematical-based assumptions as well as sophisticated algorithms. This technique is used as a powerful method for computing random issues with and without uncertain variables [16].

The heart of the UT method is how we can generate suitable examples of input variables that can maintain the proper information about the PDF of the input variables. The assumption is that x is the vector of *n*-dimensional random variables with mean $x = m$ and covariance P_{XX}. The other random variable Y is x-dependent, which is calculated by $y = f(x)$, and f can be a set of non-linear functions.

In UT, the mean and covariance of output variables Y as well as P_{YY} can be calculated applying the following steps.

Step 1: (1 + 2n) samples or sample points can be obtained by using following equations.

$$X^0 = m \quad (8)$$

$$X^k = m + \left(\sqrt{\frac{n}{1 - w^0}P_{XX}}\right)_k\ .\ k = 1.2.\ldots.n \quad (9)$$

$$X^{k+n} = m + \left(\sqrt{\frac{n}{1 - w^0}P_{XX}}\right)_k\ . \quad (10)$$
$$k + n = 1.2.\ldots.n$$

Step 2: Using following Eqs. 11-13, the relative weights to each x can be calculated based on the conditions given in Eq. 14.

$$w^0 = w^0 \quad (11)$$

$$w^k = \frac{1 - w^0}{2n}.\ k = 1.2.\ldots.n \quad (12)$$

$$w^{k+n} = \frac{1 - w^0}{2n}.\ k + n = 1.2.\ldots.n \quad (13)$$

$$\sum_{k=0}^{2n} w^k = 1 \quad (14)$$

In Eqs. 9 and 10, $\left(\sqrt{(n)/(1 - w^0)P_{xx}}\right)_k . k$ is the value of the row or column k of the second root of the matrix $\sqrt{(n)/(1 - w^0)P_{xx}}$. The second root of the matrix P means that the matrix $A = \sqrt{P}$ and $P = AA^T$. Here, w^0 is the weight assigned to point $\bar{x} = m$, which is known as the "zero points" that controls the position of the other points around the mean value of x.

Step 3: Subject to a nonlinear function, each sample point is calculated to obtain a set of sample points that are converted using Eq. 15.

$$y^k = f(X^k) \quad (15)$$

As an important note, the nonlinear function is modeled as a black box in the UT.

Step 4: The mean and the covariance of the output variable Y was calculated by applying Eqs. 16 and 17, respectively.

$$\bar{Y} = \sum_{k=0}^{2n} w^k Y^k \quad (16)$$

$$P_{YY} = \sum_{k=0}^{2n} w^k \left(Y^k - \bar{Y}\right)\left(Y^k - \bar{Y}\right)^T \quad (17)$$

The UT has two essential features: first of all, sample points are not randomly selected, but they are calculated in a way that to have a predicted mean and covariance, secondly; the weights of the selected points should not be placed in the range (1, 0), but they can have positive or negative values, which should meet the condition of Eq. 14 in the weights equal to unity [7].

2.1.2.3 Internal point method

In this section, the main steps of the Internal Point Method (IPM) as a powerful conventional method are briefly presented. The interested readers are referred to see [33] for detailed descriptions of IPM; the formulation of this nonlinear optimization constrained method is presented in Eq. 18.

$$\begin{aligned} &Min.\ \mathrm{f}(z), Subject\ \mathrm{to}\ \mathrm{h}(z) = 0 \\ &z - s_l = l \quad z + s_u = u \quad s_l \geq 0\ , s_u \geq 0 \end{aligned} \quad (18)$$

In this formulation, the operational constraints (inequality constraints) are converted to equality ones and are entered using the remaining variables in $h(z)$ [47]. The vector z contains both the original and the remaining variables. Slack variables s_l and s_u converge to equality constraints.

The constraints of Eq. 18 are eliminated by adding a logarithmic barrier function to the objective function, which is shown in Eq. 19. As a result, variables s_l and s_u should be greater than zero, and variables z can never be assumed to be on boundary values.

$$Min\ \mathrm{f}(z) - \mu.\sum_{j=1}^{n} ln\left(s_{l_j}\right) - \mu.\sum_{j=1}^{n} ln\left(s_{u_j}\right) \quad (19)$$

First, the barrier parameter of μ must be supposed to be higher than zero; the value μ^0 at the end of the iteration process should be close to zero. Thus, the Lagrange function is defined as Eq. 20.

The optimal conditions of the first-order Karush Kuhn Tucker (KKT) method for the optimization problem with the results of the Newton-Raphson method are shown in Eq. 21. The mathematical expansion to obtain Eq. 21 is presented in the Appendix.

$$\begin{aligned} L = f(z) &- \sum_{j=1}^{m} \lambda_i . h_i(z) \\ &- \mu.\sum_{j=1}^{n} ln\left(s_{l_j}\right) \\ &- \mu.\sum_{j=1}^{n} ln\left(s_{u_j}\right) \\ &- \sum_{j=1}^{n} \pi_{l_j}.\left(z_j - s_{l_j} - l_j\right) \\ &- \sum_{j=1}^{n} \pi_{u_j}.\left(z_j + s_{u_j} - u_j\right) \end{aligned} \quad (20)$$

$$\begin{bmatrix} H_z & -J^t \\ -J & 0 \end{bmatrix}\begin{bmatrix} \Delta z \\ \Delta\lambda \end{bmatrix} = -\begin{bmatrix} G_z \\ h(z) \end{bmatrix} \quad (21)$$

$$\begin{aligned} H_z = w(z.\lambda) &+ \sum_j \left(\frac{\mu}{s_{l_j}^2} + \frac{\mu}{s_{u_j}^2}\right) G_z \\ &= r(z.\lambda) \\ &+ \sum_j \left(\frac{\mu}{s_{l_j}} + \frac{\mu}{s_{u_j}}\right) r(z.\lambda) \\ &= -\nabla_z f(z) + \nabla_z h(z)^t . \lambda \end{aligned} \quad (22)$$

Eq. 22 shows the barrier parameters and the slack variables to matrix diameter elements H_z and also the gradient vector G_z. It can be seen that zero values cannot be considered for slack variables.

By solving the Eq. 21, Δz and $\Delta\lambda$ are obtained. On the other hand, $\Delta s_l, \Delta s_u,\ \Delta\pi_l$ and $\Delta\pi_u$ are obtained from Eq. 53 and Eq. 54 respectively, which are shown in the Appendix. The lengths of the steps α_p and $\alpha_d \in 0{,}1$ are calculated from Eq. 23. These equations are used to maintain the positive s_l and s_u also the proper signal π_l and π_u.

$$\begin{aligned} \alpha_p &= min\left\{\min_{\Delta s_{l_j}<0} \frac{s_{l_j}}{\left|\Delta s_{l_j}\right|}, \min_{\Delta s_{u_j}<0} \frac{s_{u_j}}{\left|\Delta s_{u_j}\right|}, 1.0\right\} \\ \alpha_d &= min\left\{\min_{\Delta\pi_{l_j}<0} \frac{\pi_{l_j}}{\left|\Delta\pi_{l_j}\right|}, \min_{\Delta\pi_{u_j}<0} \frac{-\pi_{u_j}}{\left|\Delta\pi_{u_j}\right|}, 1.0\right\} \end{aligned} \quad (23)$$

The parameter σ with the value of 0.9995 is usually added to Eqs. 24 to maintain values s and π. Then, the variable optimization problem is updated by these equations.

$$
\begin{aligned}
z &= z + \sigma.\alpha_p.\\
\Delta z s_l &= s_l + \sigma.\alpha_p.\\
\Delta s_l s_u &= s_u + \sigma.\alpha_p.\\
\Delta s_u \lambda &= \lambda + \sigma.\alpha_d.\\
\Delta\lambda\pi_l &= \pi_l + \sigma.\alpha_d.\\
\Delta\pi_l\pi_u &= \pi_u + \sigma.\alpha_d.\Delta\pi_u
\end{aligned}
\tag{24}
$$

The barrier parameter μ is updated concerning the duality gap by Eq. 25 [48]. The parameter β in Eq. 25 is introduced for control μ to improve the convergence process [49].

$$
\mu = \beta.\frac{\sum_{j=1}^{n}\left(s_{l_j}.\pi_{l_j} - s_{u_j}.\pi_{u_j}\right)}{2\,.n} \tag{25}
$$

As can be seen from Eq. 25, the product of the $s_{l_j}.\pi_{l_j}$ or $s_{u_j}.\pi_{u_j}$ when the corresponding restriction is activated leads to the inclusion of π_{l_j} or π_{u_j} to a high value while s_{l_j} or s_{u_j} cannot be worthless. The result of the multiplication $s_{l_j}.\pi_{l_j}$ or $s_{u_j}.\pi_{u_j}$ will be high, while it should be zero. This feature has caused the problem of the optimal power flow to be unstable numerically or difficult for convergence.

From Eq. 19, we can see that variables z cannot consider their limit since slack variables cannot be exactly zero, which affects the quality of the solution. As mentioned in the introduction, many of the proposed works in the literature are presented to overcome these challenges.

To solve the problem, first, the new parameter δ is added in Eq. 19. The amount of δ is always definite. In this new formulation, the convergence process is controlled by the parameter δ instead of s_l and s_u. Entering δ the logarithmic barrier function causes the slack variables are now able to reach a value of zero. During the Newton Raphson repeat process, the value of δ is independent of the parameter value γ defined in Eq. 26.

$$
\delta_{k+1} = \gamma\,.\,\delta_k \tag{26}
$$

In Eq. 26, k is the iteration number, γ is the reduction coefficient $\delta.\gamma$ is the defined parameter δ to accelerate the convergence rate. Finally, the parameter μ is corrected. The Eq. 52 of the appendix is used to reduce the barrier parameter μ, and the parameter δ for j is rewritten as Eq. 27.

$$
\begin{aligned}
2\,.n\,.\ \mu = &+\sum_{j=1}^{n}\left[s_{l_j}.\pi_{l_j} - s_{u_j}.\pi_{u_j}\right] +\\
&\delta.\sum_{j=1}^{n}\left[\pi_{l_j} - \pi_{u_j}\right]
\end{aligned}
\tag{27}
$$

The first plural term on the right of Eq. 27 is similar to the GAP known in [49] and [50]. Also, given the positive π_l and the negative π_u, the new correction that appears at the end of Eq. 47 is always positive and tends to be very small because the assumption of δ it can be seen to be a close to zero value that can be seen in the initial criteria and convergence. The value of y can be calculated from Eq. 28.

$$
\mu = \beta.\frac{\sum_{j=1}^{n}\left(s_{l_j}.\pi_{l_j} - s_{u_j}.\pi_{u_j}\right) + \delta.\sum_{j=1}^{1}\left(\pi_{l_j} - \pi_{u_j}\right)}{2\,.n} \tag{28}
$$

A parameter β is usually introduced in the calculations μ to accelerate the convergence process. When the slack variable s_{l_j} is zero, the Lagrange coefficient π_{l_j} is assumed to be significant because the optimization variable z_j is at the minimum limit. As a result, the coefficients $s_{l_j}.\pi_{l_j}$and $s_{u_j}.\pi_{u_j}$ become zero, which causes the OPF problem to be numerically stable and more straightforward to achieve convergence.

2.2 Modeling Constraints

As already mentioned, the OPF and POPF problem has consisted of both equality and inequality constraints. These constraints are detailed in this section separately.

2.2.1 Equality constraints

The power balance equations are represented by Eq. 29 and Eq. 30, for active and reactive powers, separately.

$$
\begin{aligned}
P_{G_i} - P_{D_i} - V_i\sum_{j=1}^{NB} V_j\big[&G_{ij}\,cos(\delta_{ij})\\
&+ B_{ij}\,sin(\delta_{ij})\big] = 0\ \forall\ \mathrm{i} \in \mathrm{NB}
\end{aligned}
\tag{29}
$$

$$
\begin{aligned}
Q_{G_i} - Q_{D_i} - V_i\sum_{j=1}^{NB} V_j\big[&G_{ij}\,sin(\delta_{ij})\\
&- B_{ij}\,cos(\delta_{ij})\big] = 0\ \forall\ \mathrm{i} \in \mathrm{NB}
\end{aligned}
\tag{30}
$$

Where, $\delta_{ij} = \delta_i - \delta_j$ is the difference of the voltage angles between buses i and j, NB is the number of buses, P_D and Q_D, are the active and reactive demanded loads respectively, G_{ij} is the conductance, and B_{ij} is the Susceptances of the line between buses i and j.

2.2.2 Inequality constraints

Inequality constraints in the problem reflect the constraints of operating states of equipment in the power system, as well as the constraints imposed on transmission lines and the load buses to ensure the security of the power system. The inequality constraints can be described as follows.

– Generator constraints:

$$V_{G_i}^{min} \le V_{G_i} \le V_{G_i}^{max} \ \forall\, i \in NG \tag{31}$$

$$P_{G_i}^{min} \le P_{G_i} \le P_{G_i}^{max} \ \forall\, i \in NG \tag{32}$$

$$Q_{G_i}^{min} \le Q_{G_i} \le Q_{G_i}^{max} \ \forall\, i \in NG \tag{33}$$

– Transformer constraints:

$$T_j^{min} \le T_j \le T_j^{max} \ \forall\, j \in NT \tag{34}$$

– Parallel compensator constraints:

$$Q_{C_i}^{min} \le Q_{C_i} \le Q_{C_i}^{max} \ \forall\, i \in NC \tag{35}$$

– Security constraints:

$$V_{L_p}^{min} \le V_{L_p} \le V_{L_p}^{max} \ \forall\, p \in NL \tag{36}$$

$$S_{l_q} \le S_{l_q}^{max\ \text{qnl}} \tag{37}$$

As mentioned previously, POPF is an optimization problem concluding some equality and inequality constraints. In this paper, the considered uncertainties are discussed and modeled.

2.2.3 Modeling wind power

The cost function for the i^{th} wind generator is determined, as follows [51].

$$C_{d.w.i} = d_{w.i} P_{w.i} \tag{38}$$

As an important note, the wind power unit operators schedule a certain value of energy, so the relevant penalty factors should be charged to provide the given amount in failure conditions [52]. The underestimation and overestimation costs [46] are mathematically modeled as follows.

$$C_{ue.w.i} = K_{ue.w.i} \int_{P_{w.i}}^{P_{w.r.i}} (P - P_{w.i}) f(P) dP \tag{39}$$

$$C_{ue.w.i} = K_{oe.w.i} \int_{0}^{P_{w.i}} (P_{w.i} - P) f(P) dP \tag{40}$$

Where i = 1, 2, …, n_w . $f(P)$ represents the PDF of the wind output power. The total cost of wind energy is calculated as follows.

$$COST_{w.i} = C_{d.w.i} + C_{ue.w.i} + C_{ue.w.i} \tag{41}$$

The PDF of the output power of the i^{th} wind power plant is addressed applying the following method:

Step 1: Generally, the Weibull distribution function is used to describe wind speed behavior. It needs two parameters, shape and scale. The Weibull PDF f (V_w) and the cumulative distribution function (CDF) $F(V_w)$ [53] are given as under.

$$f_{(V_w)} = \frac{K}{C}\left(\frac{V_w}{C}\right)^{k-1} e^{-(V_w/C)^K}.\ V_w > 0 \tag{42}$$

$$F(V_w) = 1 - e^{-(V_w/C)^K}.V_w > 0 \tag{43}$$

Step 2: Calculate the produced power by the wind power plant as follows.

$$P_w(V_w) = \begin{cases} 0 & V_w < V_{w.in}\ .V_w > V_{w.out} \\ \dfrac{V_w P_{w.r}}{V_{w.r} - V_{w.in}} - \dfrac{V_{w.in} P_{w.r}}{V_{w.r} - V_{w.in}} & V_{w.in} \le V_w \le V_{w.r} \\ P_{w.r} & V_{w.r} \le V_w \le V_{w.out} \end{cases} \tag{44}$$

Where V_w and $V_{w.r}$ are the speed and rated speed of the wind energy generators, respectively. $V_{w.in}$ and $V_{w.out}$ are the cut-in and cut-out speeds. K, C determines the shape and scale factors of the Weibull PDF. The PDF of the wind speed is shown in Fig. 1.

2.2.4 Probabilistic nature of Photovoltaic Cell generated energy

The generation of photovoltaic power plants is mostly influenced by weather conditions. Generally, the output power varies based on the intensity of the light. The light intensity in a short time is demonstrated by the beta distribution function [47]. The PDF can be presented by Eq. 45.

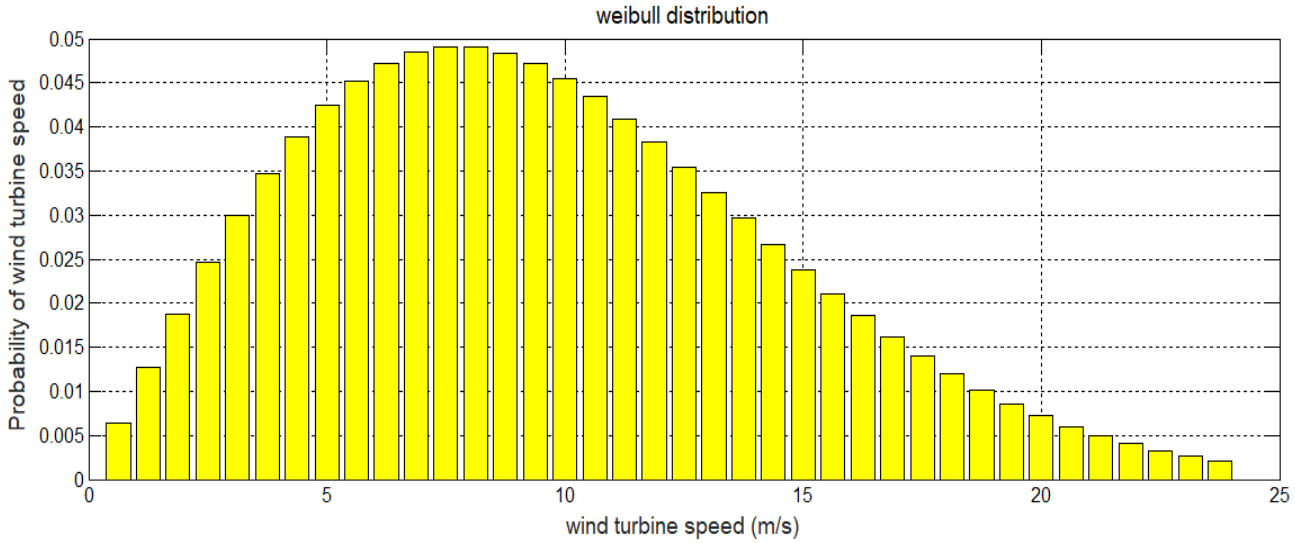

Fig. 1. PDF of wind speed (m/s)

$$f(r) = \frac{\Gamma(\alpha+\beta)}{\Gamma(\alpha)\Gamma(\beta)}\left(\frac{r}{r_{max}}\right)^{\alpha-1}\left(1-\frac{r}{r_{max}}\right)^{\beta-1} \quad (45)$$

Where α and β are Beta distribution parameters, Γ gamma function, r is the actual light intensity in a period, and r_{max} is the maximum intensity of light during a period.

The parameters of α and β can be described by mean μ and standard deviation σ of light intensity using Eqs. 46 and 47.

$$\alpha = \mu\left[\frac{\mu(1-\mu)}{\sigma^2}-1\right] \quad (46)$$

$$\beta = (1-\mu)\left[\frac{\mu(1-\mu)}{\sigma^2}-1\right] \quad (47)$$

After obtaining the light probability density function, we can calculate the output power P_M and the maximum output power $P_{M_{max}}$. P_M and $P_{M_{max}}$ were obtained through Eqs. 48 and 49, respectively.

$$P_M = r.A.\eta \quad (48)$$

$$P_{M\,max} = r_{max}.A.\eta \quad (49)$$

Where A is the photovoltaic total area array, and η is the battery efficiency. Therefore, the probability density function of the output power P_M is obtained by Eq. 50.

$$f(P_M) = \frac{\Gamma(\alpha+\beta)}{\Gamma(\alpha)\Gamma(\beta)}\left(\frac{P_M}{P_{M\,max}}\right)^{\alpha-1}\left(1-\frac{P_M}{P_{M\,max}}\right)^{\beta-1}$$

As a result, the PDF of the output power P_M is described by the Beta distribution. The PDF of the photovoltaic cells is shown in Fig. 2.

2.2.5 Probabilistic load model

In the deterministic model, the load demand in each bus is considered to be constant. Time and weather are two critical factors affecting the load. The random components of the random variables are independent. The behavioral patterns of energy consumers lead to some changes in the demanded load. These changes can be calculated by statistical analysis. As a result, the demanded load is consistently different, with a high degree of uncertainty.

In this paper, the load is considered a normal PDF with a mean value μ and standard deviation σ. Normal PDF can be accessed via Eq. 51. The form of this function is shown in Fig. 3.

$$f(P_L) = \frac{1}{\sigma\sqrt{2\pi}}exp\left(-\frac{(P_L-\mu)^2}{2\sigma^2}\right) \quad (51)$$

3. Software Simulation

The suggested techniques are programmed in MATLAB software environment and implemented on an Intel Pentium CPU 1.8 GHz PC with 8 GB RAM

3.1 The 300 – bus IEEE system

To study the utilization of the POPF analysis and the performance of the presented methods, a 300-bus IEEE system consisting of 69 generators, 300-bus, and wind turbines and solar cells were implemented [48].

Information on generators, transmission lines, and consumers is presented in [48].

Before running this system in MATLAB software, solar and wind power plants were located in various buses; in this paper, the location of the mentioned power plants is considered in buses 7 and 8, respectively. Changing the location causes changes in the reported results.

Diagram of the 300 – bus IEEE system is shown in the appendix. By comparing the four numerical and analytical methods shown in Table 1, it can be verified that MCS methods, 3-PEM, and UT methods have a close range of variations. However, according to the results, it can be seen that in the IPM, due to the existence of barrier and finite parameters limiting the range of generation, the results are more different than from methods. However, all results are still within the specified range according to the requirements of power generation.

Table 1

Comparison of the results in term of the average change in generated powers [MW]

Gen. No.	Mean active power [MW]			
	MCS	3PEM	UT	IPM
1	0.0002	0.0002	0.0002	50
2	0.0002	0.0002	0.0002	66
3	8.5646	7.6196	10.196	35
4	62.158	62.068	62.273	71
5	99.999	99.999	99.999	100
6	403.43	403.34	403.55	433
7	156.88	156.80	157.01	181
8	285.21	285.09	285.40	280
9	75.760	75.722	75.819	115
10	140.86	140.80	140.95	136
11	1983.5	1982.9	1984.5	1991
12	249.35	249.27	249.47	256
13	92.040	91.630	92.735	90
14	0.9811	0.7152	1.4994	25
15	277.50	277.42	277.63	265
16	658.67	658.49	658.93	670
17	79.993	79.971	80.028	83
18	198.53	198.48	198.62	210
19	96.523	96.496	96.561	103
20	340.38	340.26	340.59	356
21	199.09	199.03	199.20	221
22	0.0002	0.0002	0.0002	80
23	199.05	198.88	199.35	200
24	42.966	42.482	43.792	44
25	195.885	195.84	195.94	230
26	79.6980	79.679	79.724	95
27	202.972	202.88	203.11	230
28	1175.22	1174.7	1175.9	1200
29	1179.43	1178.9	1180.1	1999
30	507.291	507.21	507.38	498
31	1867.08	1866.9	1867.2	1900
32	440.492	440.41	440.56	441
33	274.907	274.86	274.94	280
34	108.184	108.16	108.20	121
35	487.474	487.40	487.55	487
36	269.621	269.57	269.67	280
37	328.436	328.38	328.49	330
38	360.766	360.71	360.83	381
39	325.727	325.67	325.78	321
40	634.352	634.25	634.46	650
41	265.625	265.58	265.67	270
42	578.008	577.92	578.10	581
43	612.284	612.18	612.40	620
44	176.164	176.13	176.18	182
45	85.6029	85.591	85.612	100
46	434.300	433.85	435.11	432
47	556.153	555.33	557.50	545
48	1138.01	1136.7	1140.2	1200
49	224.054	223.70	224.60	256
50	354.367	353.98	355.03	360
51	387.436	387.20	387.80	390
52	165.895	165.75	166.14	170
53	383.404	383.05	384.00	400
54	515.481	515.19	515.93	521
55	39.8789	39.863	39.902	81
56	71.8833	71.578	72.347	99
57	47.8626	47.847	47.884	113
58	159.177	159.14	159.21	171
59	375.723	375.67	375.78	400
60	379.667	379.60	379.75	391
61	137.529	137.49	137.56	150
62	1219.62	1218.4	1221.6	1250
63	716.004	715.77	716.38	730
64	491.081	490.92	491.33	501
65	27.9801	27.879	28.080	30
66	53.0252	52.792	53.373	70
67	49.5611	49.331	49.903	50
68	53.1748	53.155	53.204	55
69	8.50904	8.5059	8.5137	35

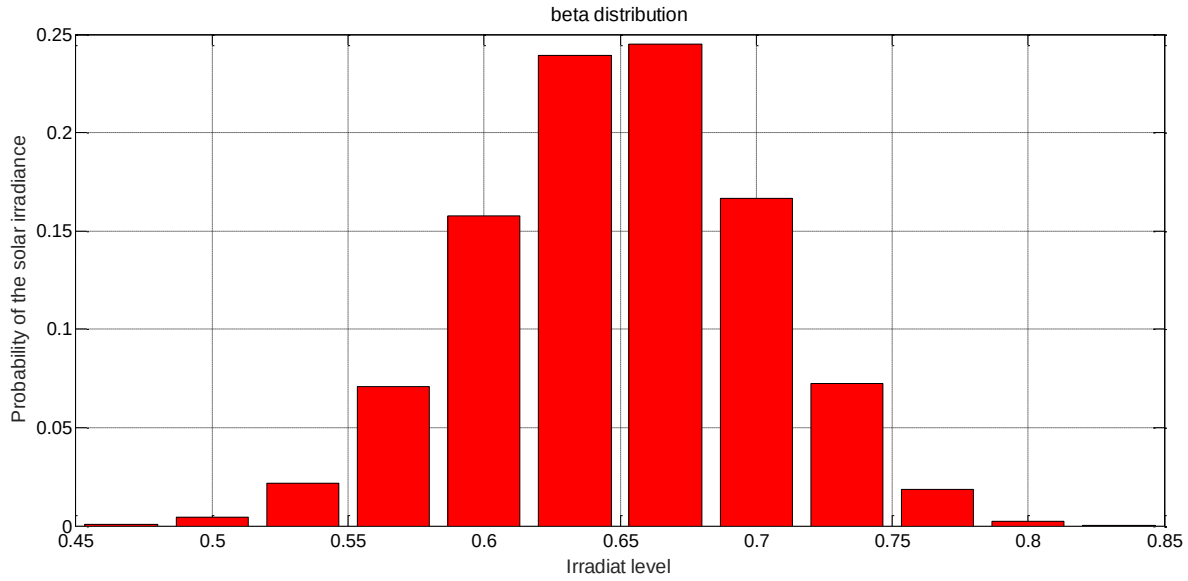

Fig. 2. PDF of photovoltaic cells (irradiance)

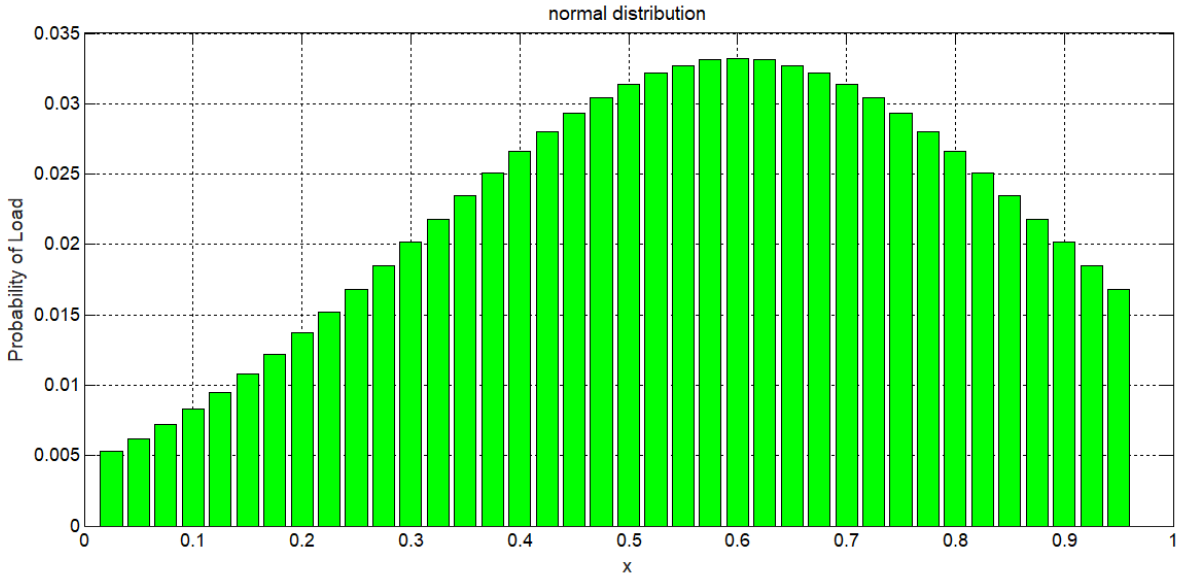

Fig. 3. Normal PDF of load (w)

As the MCS method is iterative, this method achieves the optimal solutions over a more extended period. However, the solutions are closer to real conditions. So, this method can be considered the basis for comparing the calculations.

To correct the estimation methods, in the three-point estimation method, in addition to calculating the weight for each variable of the Eqs. 18 and 19, the coefficients of skewness and kurtosis are used. These equations increase the accuracy of this method.

The skewness coefficients represent the probability distribution asymmetry and are assumed to be equal to the third-order torque. If the data are (symmetric) than the mean, then it is equal to zero. Its value is equal to an asymmetric distribution with a definite upward elongation, and it is negative for asymmetric distribution with elongation to smaller values.

Also, the kurtosis coefficient describes the sum of the peak or flatness of the probability distribution equal to the fourth-order torque. The value of this coefficient for the densities of the sharp probability and the large sequence will be higher and will be a criterion of sharpness of the standard curve. So, using the three-point estimation method is recommended.

According to the results, in the UT method, using Eqs. 23 to 32, it can be concluded that this method does not randomly select the sample points, unlike the PEMs. These points are selected to have mean values and covariance. The weights of the points should be positive and negative, according to Eq. 29. The results show that

the accuracy of this method is similar to the MCS method.

Analyzing the results in the generator voltage profile viewpoint shows that, according to Fig. 4, all of the voltages are in the predefined range. The IPM has the lowest voltage variation. These changes are in the range of 1 to 1.01 p.u. Therefore, this method has more voltage stability. The three MCS methods, the 3-PEM, and UT method, have a similar range of variations. The minimum variation range of these three methods is 0.499 p.u. for generator 23, and the maximum amount is equal to 1.05 p.u. for generators 6, 8, 11, 14, 14, 18, 19, 20, 25, 28, 31, 46, 50, 52, 59, 62 and 64.

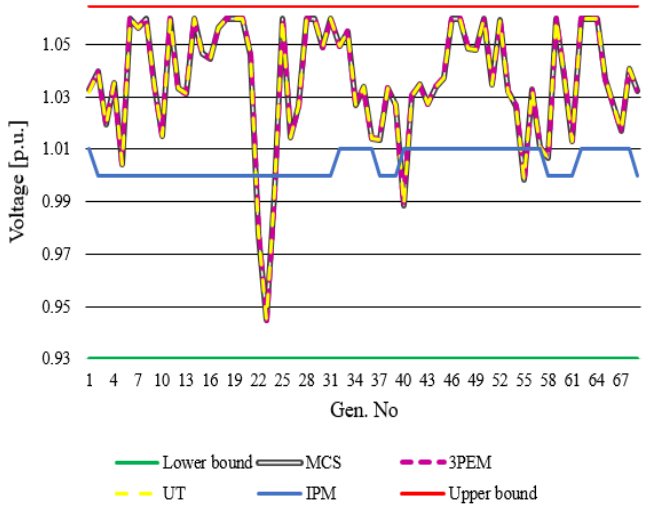

Fig. 4. Profiles of generator voltage (per unit)

The voltage variations in different buses of the network are shown in Fig. 5. In Fig. 5, the maximum and minimum range of voltage variations are specified. The minimum voltage variations in the buses are related to the IPM. The voltage variations in this method are in the range of 1 to 1.009 p.u. Other methods also have the same range of changes, and all voltage variations are also within the predefined minimum and maximum limits.

According to the results shown in Fig. 6, it can be seen that the MCS method has the highest run-time. The IPM has the lowest run-time as it uses the penalty coefficients in problem-solving. The results of other methods are between these two methods. If we select the IPM solutions as the best, in terms of running time, the run-time of 3-PEM, UT, and MCS methods will be increased equal to 10.9%, 158.9%, and 2708.8% compare to it.

Figs. 7 and 8 depict the convergence of the POPF problem in the MCS method and IPM based on the number of iterations. The starting point in these figures is the cost of the deterministic OPF problem, neglecting all uncertainties. As the figures show, the starting point for deterministic OPF is more expensive than the states which consider the uncertainties or POPF problem. These results indicate a reduction in the cost of network operation considering renewable energies.

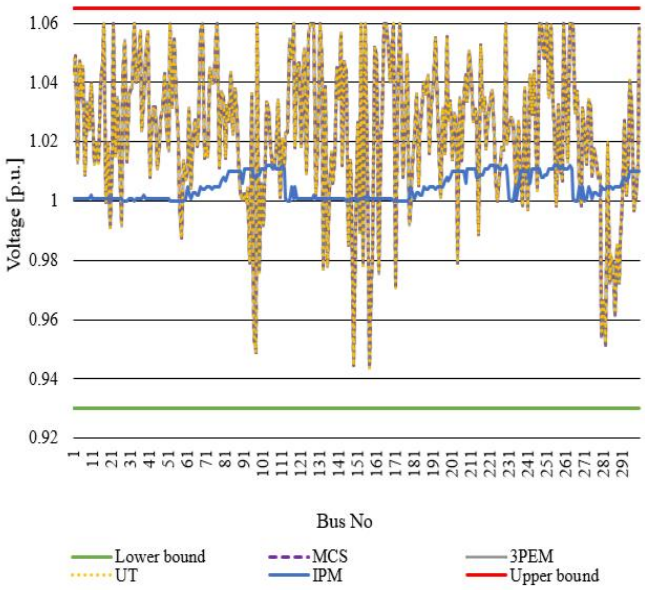

Fig. 5. Profiles of bus voltage (per unit)

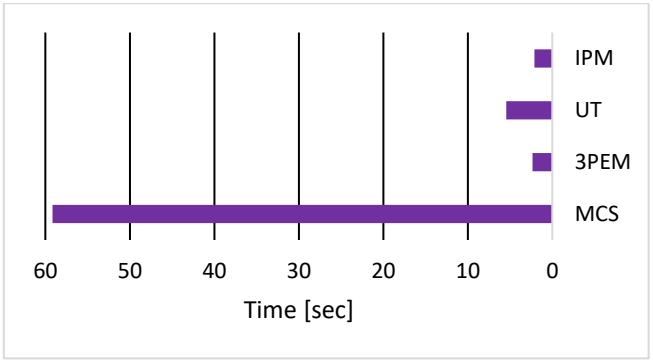

Fig. 6. The runtime of the studied methods (s)

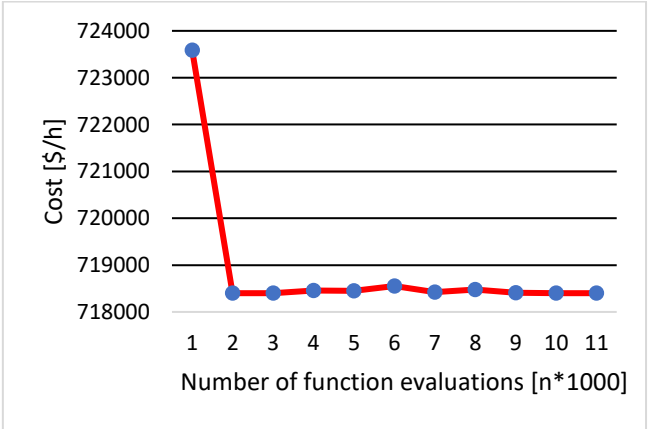

Fig. 7. Convergence curve Monte Carlo simulation method ($/h)

Fig. 7 shows the convergence diagram of the MCS method, with the wind and solar resource's penetration. The cost of OPF decreases from 723,548 ($/hr.) to

718,400 ($/hr.). When the iteration numbers are selected equal to 60,000, the final results converged to 718,400 ($/hr.).

Also, Fig. 8 shows the convergence of the IPM, which starts at 810,215 ($/hr.), reduces to 800,114 ($/hr.) By comparing Fig. 7 and Fig. 8, it can be concluded that the speed of convergence in IPM is much higher than the MCS method. However, in terms of cost optimization, the MCS method has a better solution than IPM.

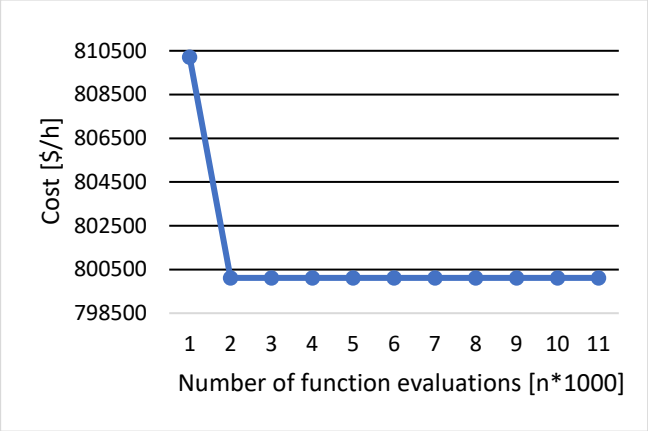

Fig. 8. Convergence curve Interior Point Method ($/h)

According to the results of Fig. 9, it can be seen that the POPF problem cost in the 3-PEM is the lowest value compared to other methods. This value is 0.071%, 0.187%, and 11.45% higher than for MCS UT, and IP methods, respectively. In 3-PEM, the number of sampling points is limited, so this method has the optimal solution.

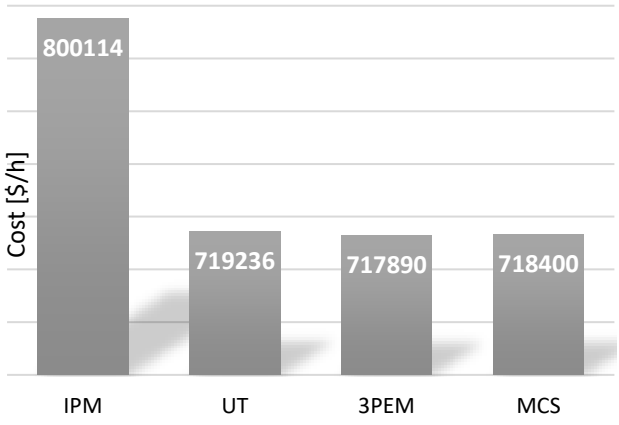

Fig. 9. The cost function of the studied methods ($/h)

3.2 An industrial 85–bus system of Kermanshah region

In this section, the case study of Kermanshah distribution network is investigated by applying the proposed probabilistic power flow techniques. For this purpose, the relevant data, including the specification of lines, load capacity, environmental information of solar power, temperature, and wind speed in 5 years are used. The total demand is 2.14 MW and 1.54 MVA. The solar radiation curve of the region and the PDF of the Kermanshah region are shown in Fig. 10. The maximum radiation level of the region is 70% and *a* and *b* coefficients of the estimated beta function are 3.215 and 2.02 by using nonlinear squares method.

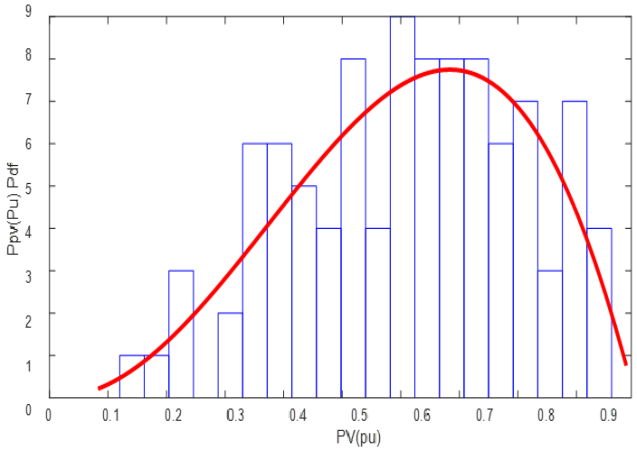

Fig. 10. Sunlight curve and PDF of Beta function

Also, the distribution wind speed of the region is shown in Fig.11, which leads to the maximum wind speed of the region equal to 12 meters per second. The Weibull and Normal distribution curves of wind speed based on the obtained data are depicted in the black and the green diagram. The PDF of the Weibull is better and more appropriate than the Normal distribution. Furthermore, the *a* and *b* coefficients of the Weibull function are 2.79 and 1.50.

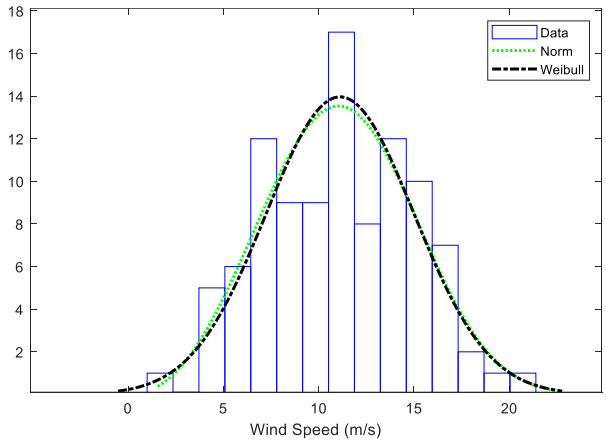

Fig.11. Wind speed curve and probability distribution function of Weibull

The curve of average seasonal load consumption profile of the distribution network during the mentioned period is shown in Fig.12.

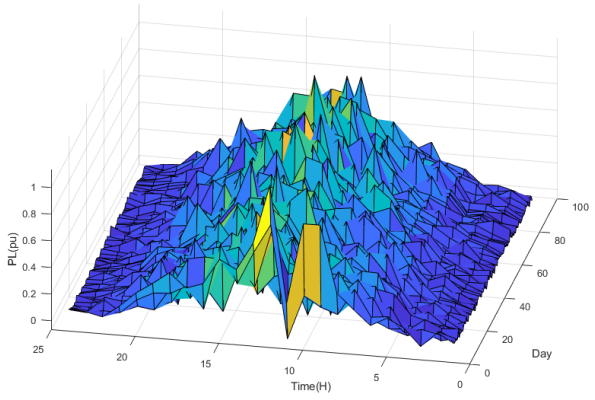

Fig. 12. The load curve profile

The estimated distribution curve for load power data is shown in Fig.13, which fits with a normal distribution with an average of 0.31 and a variance of 0.17 MW.

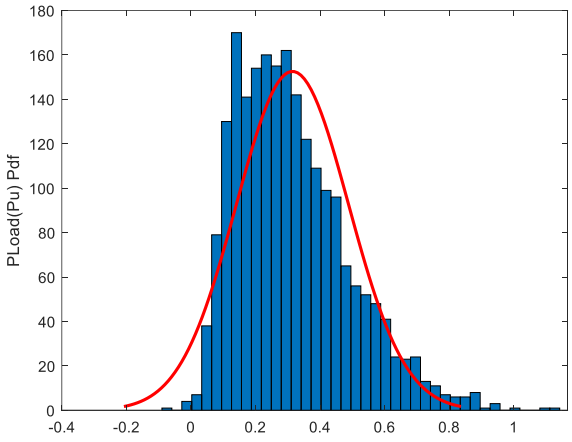

Fig. 13. Load power distribution curve

For completing the simulation process, a probabilistic scenario for resource capacity and examine the estimation of probabilistic methods is assumed. It should be noted that this scenario is intended for better operation, management, and feasibility of solar and wind resources.

In this study, we assume that the wind power plants are allocated in high-consumption industrial buses, by a capacity of 200 kW. Also, the solar generation power plants are mentioned in high-consumption industrial buses, each one by a capacity of 300 kW.

A scenario including the normal distribution function of load, wind Weibull distribution, and solar beta distribution is considered. Then the probabilistic load flow methods are investigated on the mentioned network. Here, the voltage of bus 46 in the prescience of all sources is demonstrated, which shows the magnitude between 0.9 and 1 per unit. Also, the multi-point estimation method overlaps well with the cumulative distribution of the Monte Carlo simulation method.

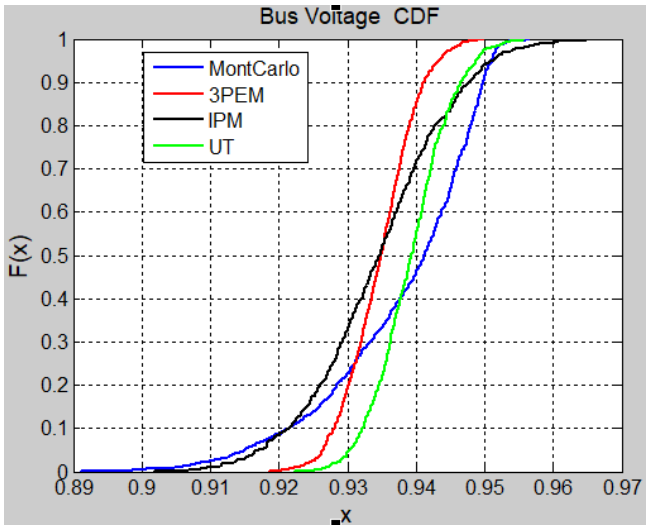

Fig. 14. The 46-bus voltage cumulative distribution function diagram

The comparative diagram of the squares of the mean voltage error of bus 46 between the Monte Carlo simulation method and other methods is shown in Fig. 15. The maximum error rate in three-point estimation, interior point, and UT methods, are equal to 0.00061, 0.0075, and 0.0076, respectively. This confirms that the error rate in the UT method is higher than the other techniques.

The comparison results are shown in Table 2. They show that the mean voltage error in the three-point estimation method is less than the other methods. Therefore, it can be concluded that the three-point estimation method is one of the most suitable methods for solving the POPF in the presence of uncertainties.

Table 2

The comparison results for the three scenarios examined

Method	Scenario
IPM	0.0075
3PEM	0.00061
UT	0.0076

4. Conclusion

In this paper, probabilistic methods for solving the POPF problem are reported in the presence of the uncertainties raised by wind power plants and solar cells. These probabilistic methods include MCS, 3PEM, UT, and IPM. Also, the uncertainty in demanded loads is modeled.

The proposed methods are simulated on a 300-bus IEEE standard network and an 85-buses feeder of Kermanshah industrial.

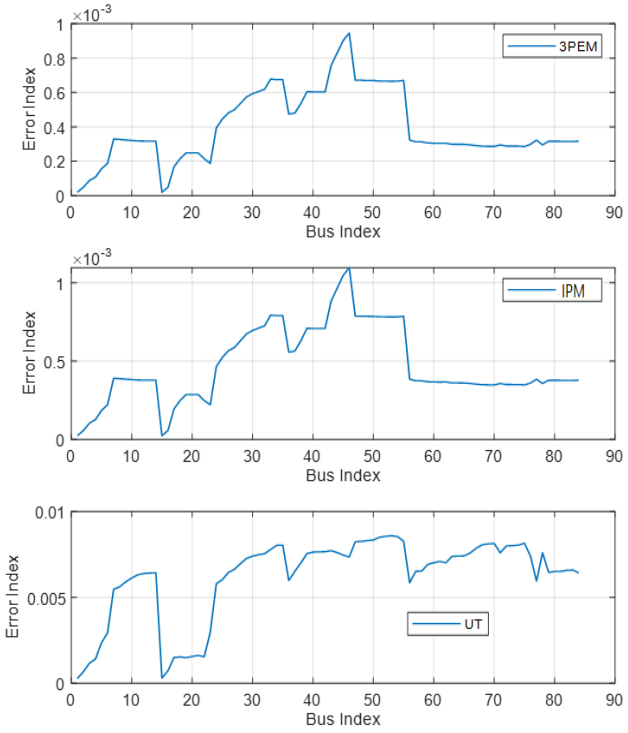

Fig.15. The comparative diagram of the squares of the mean bus voltage error

The most important findings 300-bus IEEE standard network can be classified as follows.

1. In terms of the objective function of optimizing the cost of power generation, the 3PEM has the best solutions among the other methods.
2. The MCS method and the IPM are iterative-based methods. In the case of convergence, the IPM has the fastest mode of convergence. This method converges in the same primitive repetition, but the MCS method is converged only after tens and even hundreds of iterations.
3. In terms of run time, the IPM is the fastest method, and other methods are the 3PEM, UT, and MCS, respectively.
4. Due to some limitations in the IPM, there are no oscillations in generator voltage changes in the network, so this method has a stable voltage profile.

In total, among the studied methods for the 300-buses IEEE network, the 3PEM has the optimal response time, voltage profile, and optimal cost comparing to other methods. The most important findings an 85-buses feeder of Kermanshah industrial can be classified.

These results show that the mean voltage error in the three-point estimation method for all three scenarios is less than the other studied methods. Therefore, it can be concluded that the three-point estimation method is one of the most suitable methods for solving probabilistic power distribution in the presence of uncertainties.

5. Appendix

The optimality mode of the first-order Karush Kuhn Tucker method for the Lagrangian function of Eq. 20 is obtained from the Newton-Raphson method in a nonlinear system as Eq. 52.

$$\begin{aligned}\nabla_z L = \nabla_z f(z) - J^t(z).\lambda - \pi_l - \pi_u = 0 \nabla_\lambda L \\ = -h(z) = 0 \nabla_{\pi_l} L \\ = -(z - s_l - l) = 0 \nabla_{\pi_u} L \\ = -(z + s_u - u) = 0 \nabla_{s_{l_j}} L \\ = -\frac{\mu}{s_{l_j}} + \pi_{l_j} = 0 \nabla_{s_{u_j}} L \\ = -\frac{\mu}{s_{u_j}} + \pi_{u_j} = 0\end{aligned} \quad (52)$$

According to the Newton equations, the direction of Δ for each variable is defined in Eq. 53:

$$\begin{aligned}w(z,\lambda).\Delta z - J^t(z).\Delta\lambda - \Delta\pi_l - \Delta\pi_u \\ = -\nabla_z L J(z).\Delta z \\ = -\nabla_\lambda L \Delta z - \Delta s_l \\ = 0\Delta z + \Delta s_u \\ = 0\frac{\mu}{s_{l_j}^2}\Delta s_{l_j} + \Delta\pi_{l_j} \\ = -\nabla_{s_{l_j}} L \frac{\mu}{s_{u_j}^2}\Delta s_{u_j} + \Delta\pi_{u_j} \\ = -\nabla_{s_{u_j}} L\end{aligned} \quad (53)$$

The steps of $\Delta\pi_l$ and $\Delta\pi_u$ can be shown in Eq. 54 by replacing Eq. 52in Eq. 53.

$$\begin{aligned}\Delta\pi_{l_j} = -\frac{\mu}{s_{l_j}^2}\Delta z_j + \frac{\mu}{s_{l_j}} - \pi_{l_j}\Delta\pi_{u_j} \\ = -\frac{\mu}{s_{u_j}^2}\Delta z_j + \frac{\mu}{s_{u_j}} - \pi_{u_j}\end{aligned} \quad (54)$$

The structure of the matrix (21) can be rewritten in Eq. 53 by replacing Eq. 54 in Eq. 53.

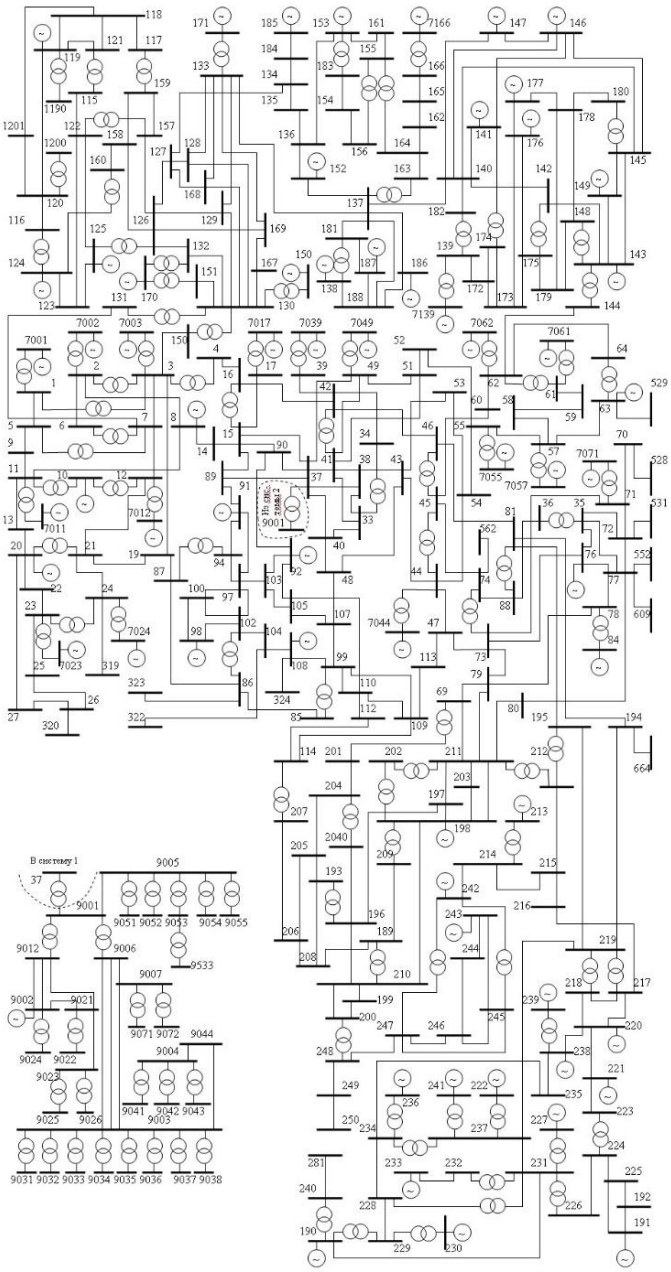

Fig. 16. Diagram of the 300 – bus IEEE system

6. References

[1] N. Gupta, "Probabilistic load flow with detailed wind generator models considering correlated wind generation and correlated loads", Renewable Energy, vol. 94, pp. 96-105, 2016.

[2] S. Shargh, B. Mohammadi-Ivatloo, H. Seyedi, and M. Abapour, "Probabilistic multi-objective optimal power flow considering correlated wind power and load uncertainties", Renewable Energy, vol. 94, pp. 10-21, 2016.

[3] M. Aien, M. Rashidinejad, and M. F. Firuz-Abad, "Probabilistic optimal power flow in correlated hybrid wind-PV power systems: A review and a new approach", Renewable and Sustainable Energy Reviews, vol. 41, pp. 1437-1446, 2015.

[4] X. Guo, R. Gong, and H. Bao, "Mixed probabilistic and interval optimal power flow considering uncertain wind power and dispatchable load", IEEJ Transactions on Electrical and Electronic Engineering, vol. 13, pp. 246-252, 2018.

[5] J. Cao and Z. Yan, "Probabilistic optimal power flow considering dependences of wind speed among wind farms by pair-copula method", International Journal of Electrical Power & Energy Systems, vol. 84, pp. 296-307, 2017.

[6] P. Bie, B. Zhang, H. Li, W. Deng, and J. Wu, "Probabilistic power flow using improved Monte Carlo simulation method with correlated wind sources", in Seventh International Conference on Electronics and Information Engineering, pp. 1041-1046, 2017.

[7] M. Aien, A. Hajebrahimi, and M. Fotuhi-Firuzabad, "A comprehensive review on uncertainty modeling techniques in power system studies", Renewable and Sustainable Energy Reviews, vol. 57, pp. 1077-1089, 2016.

[8] Y. Yuan, J. Zhou, P. Ju, and J. Feuchtwang, "Probabilistic load flow computation of a power system containing wind farms using the method of combined cumulants and Gram–Charlier expansion", IET renewable power generation, vol. 5, pp. 448-454, 2011.

[9] C. Chen, W. Wu, B. Zhang, and H. Sun, "Correlated probabilistic load flow using a point estimate method with Nataf transformation", International Journal of Electrical Power & Energy Systems, vol. 65, pp. 325-333, 2015.

[10] X. Ai, J. Wen, T. Wu, and W.-J. Lee, "A discrete point estimate method for probabilistic load flow based on the measured data of wind power", IEEE Transactions on Industry Applications, vol. 49, pp. 2244-2252, 2013.

[11] D. Villanueva, J. L. Pazos, and A. Feijoo, "Probabilistic load flow including wind power generation", IEEE Transactions on Power Systems, vol. 26, pp. 1659-1667, 2011.

[12] J. Usaola, "Probabilistic load flow in systems with wind generation", IET generation, transmission & distribution, vol. 3, pp. 1031-1041, 2009.

[13] J. Usaola, "Probabilistic load flow with correlated wind power injections", Electric Power Systems Research, vol. 80, pp. 528-536, 2010.

[14] J. M. Morales, L. Baringo, A. J. Conejo, and R. Mínguez, "Probabilistic power flow with correlated wind sources", IET generation, transmission & distribution, vol. 4, pp. 641-651, 2010.

[15] M. N. Kabir, Y. Mishra, and R. Bansal, "Probabilistic load flow for distribution systems with uncertain PV generation", Applied Energy, vol. 163, pp. 343-351, 2016.

[16] M. Aien, M. Fotuhi-Firuzabad, and F. Aminifar, "Probabilistic load flow in correlated uncertain environment using unscented transformation", IEEE Transactions on Power Systems, vol. 27, pp. 2233-2241, 2012.

[17] E. Rosenblueth, "Point estimates for probability moments", Proceedings of the National Academy of Sciences, vol. 72, pp. 3812-3814, 1975.

[18] J. He and G. Sällfors, "An optimal point estimate method for uncertainty studies", Applied mathematical modelling, vol. 18, pp. 494-499, 1994.

[19] H. Hong, "An efficient point estimate method for probabilistic analysis", Reliability Engineering & System Safety, vol. 59, pp. 261-267, 1998.

[20] G. Verbic and C. A. Canizares, "Probabilistic optimal power flow in electricity markets based on a two-point estimate method", IEEE Transactions on Power Systems, vol. 21, pp. 1883-1893, 2006

[21] M. Aien, M. Fotuhi-Firuzabad, and M. Rashidinejad, "Probabilistic optimal power flow in correlated hybrid wind–photovoltaic power systems", IEEE transactions on smart grid, vol. 5, pp. 130-138, 2014.

[22] M. Aien, M. G. Khajeh, M. Rashidinejad, and M. Fotuhi-Firuzabad, "Probabilistic power flow of correlated hybrid wind-photovoltaic power systems", IET renewable power generation, vol. 8, pp. 649-658, 2014.

[23] N. Karmarkar, "A new polynomial-time algorithm for linear programming", in Proceedings of the sixteenth annual ACM symposium on Theory of computing, pp. 302-311, 1984.

[24] V. H. Quintana, G. L. Torres, and J. Medina-Palomo, "Interior-point methods and their applications to power systems: a classification of publications and software codes", IEEE Transactions on Power Systems, vol. 15, pp. 170-176, 2000.

[25] P. Arboleya, C. Gonzalez-Moran, and M. Coto, "Modeling FACTS for power flow purposes: A common framework", International Journal of Electrical Power & Energy Systems, vol. 63, pp. 293-301, 2014.

[26] A. B. Babić, A. T. Sarić, and A. Ranković, "Transmission expansion planning based on Locational Marginal Prices and ellipsoidal approximation of uncertainties", International Journal of Electrical Power & Energy Systems, vol. 53, pp. 175-183, 2013.

[27] E. J. Oliveira, L. W. Oliveira, J. Pereira, L. M. Honório, I. C. S. Junior, and A. Marcato, "An optimal power flow based on safety barrier interior point method", International Journal of Electrical Power & Energy Systems, vol. 64, pp. 977-985, 2015.

[28] M. G. Breitfeld and D. F. Shanno, "Computational experience with penalty-barrier methods for nonlinear programming", Annals of Operations Research, vol. 62, pp. 439-463, 1996.

[29] J. T. Saraiva and V. Miranda, "Evaluation of the performance of a fuzzy optimal power flow algorithm", in Proceedings of MELECON'94. Mediterranean Electrotechnical Conference, pp. 897-900, 1994.

[30] R.-H. Liang and J.-H. Liao, "A fuzzy-optimization approach for generation scheduling with wind and solar energy systems", IEEE Transactions on Power Systems, vol. 22, pp. 1665-1674, 2007.

[31] A. Soroudi and M. Ehsan, "A possibilistic–probabilistic tool for evaluating the impact of stochastic renewable and controllable power generation on energy losses in distribution networks—a case study", Renewable and Sustainable Energy Reviews, vol. 15, pp. 794-800, 2011.

[32] Y. Li, W. Li, W. Yan, J. Yu, and X. Zhao, "Probabilistic optimal power flow considering correlations of wind speeds following different distributions", IEEE Transactions on Power Systems, vol. 29, pp. 1847-1854, 2014.

[33] C. S. Saunders, "Point estimate method addressing correlated wind power for probabilistic optimal power flow", IEEE Transactions on Power Systems, vol. 29, pp. 1045-1054, 2013.

[34] M. Li, Q. Wu, T. Ji, and H. Rao, "Stochastic multi-objective optimization for economic-emission dispatch with uncertain wind power and distributed loads", Electric Power Systems Research, vol. 116, pp. 367-373, 2014.

[35] E. Zio, M. Delfanti, L. Giorgi, V. Olivieri, and G. Sansavini, "Monte Carlo simulation-based probabilistic assessment of DG penetration in medium voltage distribution networks", International Journal of Electrical Power & Energy Systems, vol. 64, pp. 852-860, 2015.

[36] Y. Zhao, F. Fan, J. Wang, and K. Xie, "Uncertainty analysis for bulk power systems reliability evaluation using Taylor series and nonparametric probability density estimation", International Journal of Electrical Power & Energy Systems, vol. 64, pp. 804-814, 2015.

[37] C. Delgado and J. Domínguez-Navarro, "Point estimate method for probabilistic load flow of an unbalanced power distribution system with correlated wind and solar sources", International Journal of Electrical Power & Energy Systems, vol. 61, pp. 267-278, 2014.

[38] X. Li, J. Cao, and D. Du, "Probabilistic optimal power flow for power systems considering wind uncertainty and load correlation", Neurocomputing, vol. 148, pp. 240-247, 2015.

[39] B. Li, S. Muhammad, B. Qi, R. Muhammad, I. Rabiul, and M. US, "Probabilistic Power Flow Model to Study Uncertainty in Power System Network Based Upon Point Estimation Method", American Journal of Electrical Power and Energy Systems, vol. 6, pp. 64-71, 2017.

[40] H. Ahmadi and H. Ghasemi, "Probabilistic optimal power flow incorporating wind power using point estimate methods", in 2011 10th International Conference on Environment and Electrical Engineering, pp. 1-5, 2011.

[41] F. Jabari, H. Seyedi, S. Najafi Ravadanegh, and B. Mohammadi-Ivatloo, "Multi-objective optimal preventive islanding based on stochastic backward elimination strategy considering uncertainties of loads and wind farms", International Transactions on Electrical Energy Systems, vol. 27, p. e2451, 2017.

[42] A. B. Krishna, N. Gupta, K. Niazi, and A. Swarnkar, "Probabilistic power flow in radial distribution systems using point estimate methods", in 2017 4th International Conference on Advanced Computing and Communication Systems (ICACCS), pp. 1-6, 2017.

[43] P. P. Biswas, P. N. Suganthan, R. Mallipeddi, and G. A. Amaratunga, "Optimal power flow solutions using differential evolution algorithm integrated with effective constraint handling techniques", Engineering Applications of Artificial Intelligence, vol. 68, pp. 81-100, 2018.

[44] S. Pajic, "Sequential quadratic programming-based contingency constrained optimal power flow", Master Thesis, Worcester Polytechnic Institute USA, 2003.

[45] M. Aien, M. Rashidinejad, and M. Fotuhi-Firuzabad, "On possibilistic and probabilistic uncertainty assessment of power flow problem: A review and a new approach", Renewable and Sustainable Energy Reviews, vol. 37, pp. 883-895, 2014.

[46] J. Zhao, F. Wen, Z. Y. Dong, Y. Xue, and K. P. Wong, "Optimal dispatch of electric vehicles and wind power using enhanced particle swarm optimization", IEEE Transactions on industrial informatics, vol. 8, pp. 889-899, 2012.

[47] N. Nikmehr and S. N. Ravadanegh, "Heuristic probabilistic power flow algorithm for microgrids operation and planning", IET generation, transmission & distribution, vol. 9, pp. 985-995, 2015.

[48] I. Dabbagchi, and R. Christie, "Power systems test case archive", University of Washington, http://www.ee.washington.edu/research/pstca (accessed on 01 June 2020).

[49] G. Irisarri, X. Wang, J. Tong, and S. Mokhtari, "Maximum loadability of power systems using interior point nonlinear optimization method", IEEE Transactions on Power Systems, vol. 12, pp. 162-172, 1997.

[50] Y. C. Wu, A. S. Debs, and R. E. Marsten, "A direct nonlinear predictor-corrector primal-dual interior point algorithm for optimal power flows", IEEE Transactions on Power Systems, vol. 9, pp. 876-883, 1994.

[51] M. J. Morshed, J. B. Hmida, and A. Fekih, "A probabilistic multi-objective approach for power flow optimization in hybrid wind-PV-PEV systems", Applied Energy, vol. 211, pp. 1136-1149, 2018.

[52] G. Ren, J. Liu, J. Wan, Y. Guo, and D. Yu, "Overview of wind power intermittency: Impacts, measurements, and mitigation solutions", Applied Energy, vol. 204, pp. 47-65, 2017.

[53] H. W. Li, A. A. Zhang, and Z. M. Zhao, "Three-phase power flow solution for weakly meshed distribution system with multi-transformer branches", Power System Protection and Control, vol. 40, pp. 11-16, 2012.

